

Lifshitz phase transitions in the ferromagnetic regime of the Kondo lattice model

Denis Golež¹ and Rok Žitko^{1,2}

¹*Jožef Stefan Institute, Jamova 39, SI-1000 Ljubljana, Slovenia*

²*Faculty for Mathematics and Physics, University of Ljubljana, Jadranska 19, SI-1000 Ljubljana, Slovenia*

(Received 10 January 2013; revised manuscript received 26 June 2013; published 30 August 2013)

We establish the low-temperature phase diagrams of the spin-1/2 and spin-1 Kondo lattice models as a function of the conduction-band filling n and the exchange coupling strength J in the regime of ferromagnetic effective exchange interactions ($n \lesssim 0.5$, $J/D \lesssim 2$). We show that both models have several distinct ferromagnetic phases separated by continuous Lifshitz transitions of the Fermi-pocket vanishing or emergence type: one of the phases has a true gap in the minority band (half metal with magnetization rigidity), the others only a pseudogap. The spin-1/2 model has the half-metal phase, two topologically different pseudogap phases, and a paramagnetic state for very large J . The spin-1 model has the half-metal phase and a single pseudogap phase with an electron pocket. We find that, quite generically, ferromagnetism and Kondo screening coexist rather than compete both in spin-1/2 and spin-1 models. We establish the hysteretic behavior of the systems in an external magnetic field: spin-flop transitions preempt further Lifshitz transitions at finite magnetic field. We establish a “ferromagnetic Doniach diagram”: in the spin-1/2 model the Curie temperature peaks near $J/D \approx 1.2$ and goes to zero, while in the spin-1 model it saturates.

DOI: [10.1103/PhysRevB.88.054431](https://doi.org/10.1103/PhysRevB.88.054431)

PACS number(s): 71.27.+a, 72.15.Qm, 75.20.Hr, 75.30.Kz

I. INTRODUCTION

Materials with competing interactions, such as many lanthanide and actinide compounds known as the heavy-fermion compounds, have complex low-temperature phase diagrams with different ground states.^{1–6} The Kondo lattice model (KLM)^{7–9} describes a conduction band of itinerant electrons and a lattice of local moments on f shells, coupled at each site by an antiferromagnetic exchange interaction J . For large J , the moments are screened. The resulting paramagnetic state has Fermi-liquid properties with strongly renormalized parameters. For small J , the conduction-band electrons are carriers of long-range magnetic interactions and the moments order. The two regimes are separated by a quantum phase transition at critical J^* , as described by the Doniach diagram,¹⁰ originally proposed to describe the unexpectedly weak antiferromagnetic behavior of some cerium compounds. While the Kondo temperature is an exponentially increasing function of J , $T_K \propto \exp(-1/\rho J)$, the Néel temperature increases at first quadratically with J , but then it peaks and decreases to zero at J^* as the Kondo screening takes over. Here ρ is the unrenormalized conduction-band density of states at the Fermi level. The simplest version of the KLM with spin-1/2 moments indeed has an antiferromagnetic (AFM) ground state (Néel order) for small J near half filling.^{11,12} The nature of the phase transition at J^* has been investigated using a variety of methods, the most accurate of which confirm that the transition is second order (quantum critical) and indicate that it involves a change of the Fermi surface topology.^{13–15} In the spin-1 KLM, there is no phase transition at half filling and the AFM phase extends to large values of J .

While most cerium compounds show AFM order, some are ferromagnetic (FM): CeRu₂Ge₂,¹⁶ CeIn₂,^{17,18} and CeRu₂Al₂B.¹⁹ A number of uranium and neptunium heavy-fermion materials are also FM: UTe,²⁰ UCu_{0.9}Sb₂,²¹ UCu_{0.5}Sb₂,²² NpNiSi₂,²³ Np₂PdGa₃,²⁴ and UCu₂Si₂.²⁵ In addition, there are strong indications of robust coexistence of the Kondo effect and ferromagnetism, in particular in U compounds. In Refs. 25–29 it has been proposed that an appropriate

minimal model for this behavior is the spin-1 version of the KLM, where in the mean-field picture the conduction-band electrons underscreen the local moments, while the residual moments order ferromagnetically. FM order appears for low and moderate electron filling n in the conduction band, $n \lesssim 0.5$.^{26,30–33} Mean-field analysis predicts two phases: for small J the stable phase is a FM regular metal, while for large J there is a transition to a FM heavy metal. Dynamical mean-field theory (DMFT) calculations demonstrated that the spin-1/2 KLM also has a FM order coexisting with (incomplete) Kondo screening.³⁴ Furthermore, this phase is a half metal with gapped minority-spin band, and a commensurability condition relates the magnetization to filling n ³⁴ due to completely filled minority-spin lower band.^{35,36} A recent mean-field analysis of the spin-1/2 model suggested the presence of several different ferromagnetic phases.³⁷ So far, however, a single FM phase has been identified in the DMFT calculations.^{32,33}

These findings open a number of questions: What is the relationship between ferromagnetism and Kondo screening: Do they compete or coexist? If there is some degree of competition, how does it manifest? What is the minimal model for studying these effects, spin-1/2 or spin-1 KLM? Is there a quantum phase transition between different FM states also in the spin-1/2 model? What is the nature of these transitions and what are their experimental signatures? Finally, which aspects of the static mean-field analysis³⁸ are correct and which must be revised in more accurate dynamical treatment? To answer these questions we have performed extensive DMFT³⁹ calculations using the numerical renormalization group (NRG) as the impurity solver,^{40–45} as well as static mean-field calculations for both models.³⁸

II. MODEL AND METHOD

We consider the Kondo lattice model

$$\mathcal{H} = \sum_{\mathbf{k}\sigma} (\epsilon_{\mathbf{k}} - \mu) c_{\mathbf{k}\sigma}^\dagger c_{\mathbf{k}\sigma} + J \sum_i \mathbf{s}_i \cdot \mathbf{S}_i, \quad (1)$$

which describes a single-orbital conduction band with dispersion $\omega = \epsilon_k$, and a lattice of local moments described by the spin- S operators \mathbf{S}_i ; \mathbf{s}_i is the conduction-band spin-density at site i , and J is the antiferromagnetic Kondo exchange coupling ($J > 0$). We focus on the Bethe lattice that has a semicircular density of states with bandwidth $2D$, but the results are generic.

A. Static mean-field theory

The static mean-field approach to interacting models consists of splitting the interaction part of the Hamiltonian (i.e., the quartic terms) as $AB \approx A\langle B \rangle + \langle A \rangle B - \langle A \rangle \langle B \rangle$, where A and B are quadratic in creation and annihilation operators. The spin-1/2 Kondo lattice model has been studied using this approach in a number of works.^{36,46,47} They have proposed the following decoupling of the $\mathbf{S} \cdot \mathbf{s}$ coupling term:

$$\mathbf{s} \cdot \mathbf{S} = \left(\frac{1}{2}c^\dagger \sigma c\right) \cdot \left(\frac{1}{2}f^\dagger \sigma f\right) = -3/4\chi^{0\dagger}\chi^0 + 1/4\chi^\dagger \cdot \chi, \quad (2)$$

where

$$\chi^\mu = \frac{1}{\sqrt{2}} \sum_{\alpha, \beta} f_\alpha^\dagger \sigma_\alpha^\mu c_\beta. \quad (3)$$

Here c, f are annihilation operators for itinerant and localized electrons, respectively, and the spin indexes α and β range over spin up and down. The index μ ranges over 0, 1, 2, 3; the operator σ^0 is the identity, while other σ^i are the Pauli matrices. These operators are complete in the spin sector $1/2 \otimes 1/2 = 1 \oplus 0$.

We find that the exchange term in the spin-1 Kondo lattice model, where \mathbf{S} is spin-1 operator, can be decomposed as

$$\mathbf{s} \cdot \mathbf{S} = - \sum_{i=1}^2 \chi_{d,i}^\dagger \chi_{d,i} + (1/2) \sum_{i=1}^4 \chi_{q,i}^\dagger \chi_{q,i}, \quad (4)$$

where $\chi_{d,i}(\chi_{q,j})$ are the doublet ($i = 1, 2$) and the quadruplet ($j = 1, 2, 3, 4$) sets of operators under the spin $SU(2)$ symmetry, namely,

$$\begin{aligned} \chi_{d,1} &= -\sqrt{1/3}c_\downarrow^\dagger f_0 - \sqrt{2/3}c_\uparrow^\dagger f_1, \\ \chi_{d,2} &= \sqrt{2/3}c_\downarrow^\dagger f_{-1} + \sqrt{1/3}c_\uparrow^\dagger f_0, \\ \chi_{q,1} &= -c_\uparrow^\dagger f_{-1}, \\ \chi_{q,2} &= -\sqrt{1/3}c_\downarrow^\dagger f_{-1} + \sqrt{2/3}c_\uparrow^\dagger f_0, \\ \chi_{q,3} &= \sqrt{2/3}c_\downarrow^\dagger f_0 - \sqrt{1/3}c_\uparrow^\dagger f_1, \\ \chi_{q,4} &= -c_\downarrow^\dagger f_1. \end{aligned} \quad (5)$$

After this decoupling, the standard mean-field analysis is performed, the details of which are described in the Supplemental Material.³⁸

B. Dynamical mean-field theory

The DMFT is exact in the limit of infinite dimensions and is a good approximation in finite dimensions for problems where the interactions are local and spatial fluctuations may be neglected.³⁹ Compared to the static mean-field analysis, the DMFT correctly takes into account local quantum fluctuations and the Kondo physics. The spatial correlations are, however, still treated at the static mean-field level.

The impurity solver used in this work, the NRG (numerical renormalization group), can handle problems at arbitrarily low temperatures and has good spectral resolution for dynamic quantities calculated directly on the real-frequency axis. Recent comparisons of DMFT calculations using the exact (up to stochastic noise) continuous-time quantum Monte Carlo simulations and using the NRG have established that the results agree to high degree in the regime where comparisons can be made.⁴⁸

III. RESULTS

A. Phase diagrams

In Fig. 1 we present the main result of this work: the phase diagrams of the spin-1/2 and spin-1 KLM as a function of n and J . For *both* spins we find several different ferromagnetic phases. Phase A corresponds to the ferromagnetic half-metal phase described by Peters *et al.*³⁴ The corresponding spin-resolved spectral functions for the $S = 1$ model are shown in Fig. 2, top panel. The minority spin band is gapped,³⁴ while the majority band exhibits the weak hybridization pseudogap characteristic of the Kondo lattice systems.^{50,51} Phase B at small J is not gapped, but there is a pronounced pseudogap just below the Fermi level in the minority band, Fig. 2, bottom panel. The spectral functions for the $S = 1/2$ model are qualitatively the same. The spectra thus suggest the occurrence of a Lifshitz transition at J^* : there is no change in the symmetry, but the Fermi surface of the minority band shrinks to a point and disappears as one goes from phase B to A. We emphasize that the two phases exist both for spin-1/2 and for spin-1 models and have similar properties; clearly, within the DMFT, the *value of the spin does not play a crucial role in the BA transition*. J^* is a nonmonotonic function of n that peaks at $n \sim 0.2$ and $n \sim 0.25$, respectively. Near $n \sim 0.4$ we observe change of behavior in the small- J phase. For $S = 1/2$ KLM,

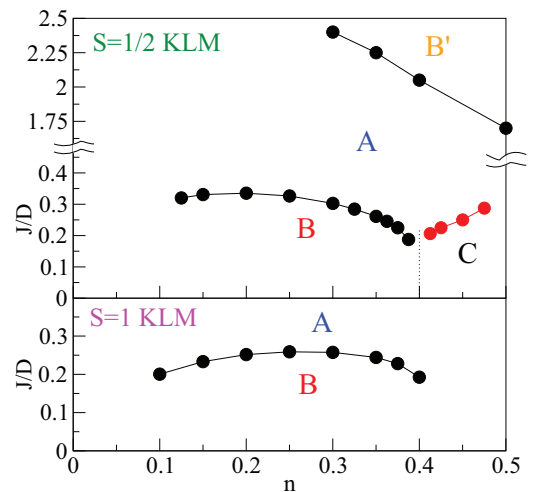


FIG. 1. (Color online) Phase diagrams of spin-1/2 and spin-1 Kondo lattice models for $n < 0.5$. Phase A is a ferromagnetic half-metal phase with strong Kondo effect where the minority band is gapped. Phases B and B' are itinerant ferromagnetic phases with a pseudogap. Phase C for the spin-1/2 model indicates the region with charge order (Ref. 49). For very small n , the calculations fail to converge.

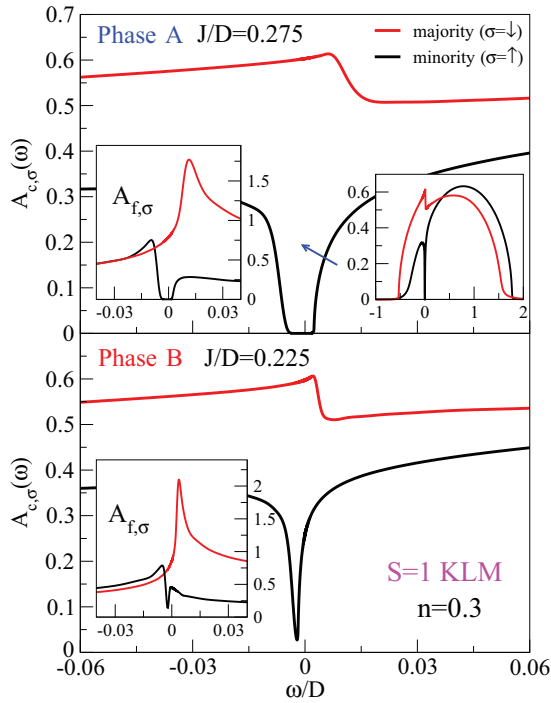


FIG. 2. (Color online) Spin-resolved conduction-band local spectral functions $A_{c,\sigma}$ for the spin-1 KLM in the ferromagnetic half-metal phase (A) and in the itinerant ferromagnetic phase (B). The arrow indicates the main effect of decreasing interaction J : the lower edge of the upper hybridized band shifts to lower frequencies. The left insets in both panels show the f -level spectral functions $A_{f,\sigma}$ defined through the imaginary part of the scattering T matrix. The right inset in the upper panel shows the spectral functions in the full frequency interval.

this is the parameter regime where charge order occurs,^{33,49} but it is not allowed for in our calculations.

In Fig. 3 we plot the magnetization and the quasiparticle renormalization factor

$$Z_\sigma = \left[1 - \frac{\partial}{\partial \omega} \Sigma_\sigma(\omega) \Big|_{\omega=\mu} \right]^{-1} \quad (6)$$

as a function of J across the BA transition. The frozen magnetization in phase A is given by a generalization of the spin-1/2 KLM result from Refs. 34–36:

$$m_S = (2S - n)/2. \quad (7)$$

At transition, the magnetization is continuous with a change of slope in m_f . This is in disagreement with the static mean-field analysis for $S = 1$ which predicts a jump.²⁷ The factors Z_σ for both spin orientations are continuous and finite across the transition (in the minority band of phase A there are no quasiparticles, but Z_σ can formally still be defined). There is thus no criticality in this spin-selective metal-insulator transition, which may be identified as a *continuous Lifshitz transition of the Fermi-pocket vanishing type*.^{35,36,52–55} The Fermi surface topology is continuous with no reorganization. Deep in the phase A, the majority electrons become weakly correlated (Z has a value of order 0.5).

For very large J , in the spin-1/2 model (but not for spin-1) there is another Lifshitz transition to a non-gapped phase⁵⁶

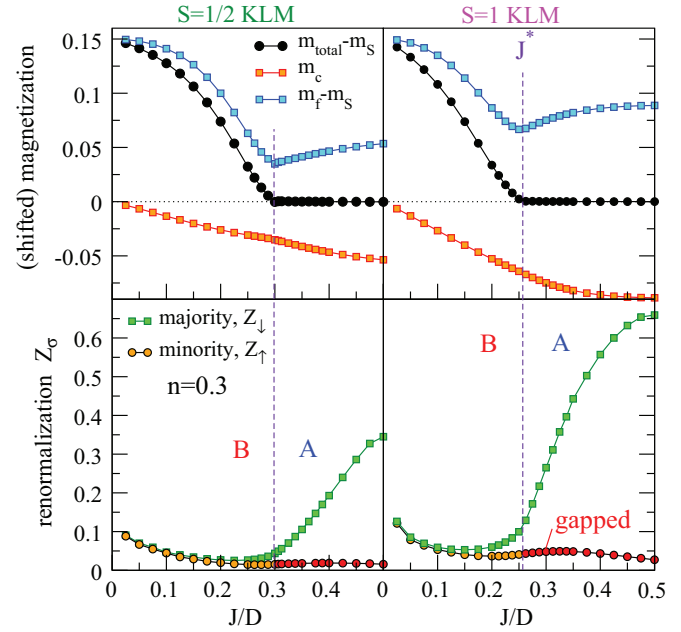


FIG. 3. (Color online) Total, conduction-band c -level, and localized f -level magnetizations (top panels) and the spin-dependent quasiparticle renormalization factors Z_σ (bottom panels) across the phase transition, indicated by the vertical dashed lines. The magnetization is here defined as the expectation value of the spin operator without the $-g\mu_B$ factor: $m_f = \langle S_z \rangle$, $m_c = (n_\uparrow - n_\downarrow)/2$, and $m_{\text{total}} = m_f + m_c$. In the plots, m_{total} and m_f are shifted by m_S defined in Eq. (7).

that we denote as B' . While in the BA transition the chemical potential is located at the *bottom of the upper hybridized band*, in the AB' transition the chemical potential is located at the *top of the lower hybridized band* at the transition point. In other words, while BA corresponds to the vanishing of the electron pocket, AB' corresponds to the emergence of the hole pocket. For even larger J , the system eventually becomes paramagnetic (for $n = 0.3$ at $J/D = 3.4$).

The static mean-field theory for $S = 1/2$ also predicts distinct phases^{37,38} which roughly correspond to B, A, and B' . The exact treatment of quantum fluctuations in DMFT leads, however, to a number of differences: (i) The small- J phase B is not pure ferromagnetic, but there is a coexistence with the Kondo effect. In the static MF treatment only a pure ferromagnetic solution is stable, and the phase transition from the corresponding phases A to B is of the first order;⁵⁴ for details see the Supplemental Material.³⁸ (ii) The Lifshitz transitions are all continuous: there are no jumps in any of the results. (iii) Deep inside phases B and B' there are pseudogaps rather than gaps. This is due to the nonzero imaginary part of the self-energy in DMFT, i.e., due to correlation effects. The most surprising outcome of the DMFT calculations is, in fact, the gradual emergence of true gaps from pseudogaps as the gapped phase A is approached from B or from B' , while the static MF results are closer to the rigid-band picture.

We note that the phases B and B' are not continuously connected, but separated by two topological Lifshitz phase transitions. The Lifshitz transitions have been intensely studied

in the context of metamagnetism in the paramagnetic phase of the Kondo lattice systems exposed to a strong external magnetic field,^{35,36,54,55} where with increasing field the pseudogap in the PM phase of the KLM becomes a gap for the minority band, while the majority band remains gapless. From the continuity of numerical results it can be established that the low-field phase is topologically equivalent to type B' and the strong-field gapped phase to type A, while for extremely large fields the systems ends up in a state of type B. More detailed analysis is in progress.

Does the existence of multiple phases indicate a competition between the exchange interaction and the Kondo effect? Some degree of antagonism is suggested by the fact that the f -shell magnetization m_f has a minimum at the BA Lifshitz point where both tendencies are expected to be equally strong and, furthermore, it could be argued that m_f increases with J in phase A only because Kondo screening is rendered incomplete by the opening and widening of the gap. Nevertheless, this competition does not imply mutual exclusion, and most results rather support the notion of robust coexistence.

B. Magnetization curves and thermodynamics

Experimentally the phases can be distinguished by their magnetization curves. In phase A, m_{total} remains pinned to m_S for a finite range of the field strength, while in phase B the susceptibility dM/dB near zero field is finite; see Fig. 4. For a sufficiently strong field, a gap opens in the minority band in phase B, too. This effect can be understood within a rigid-band picture, which holds to a first (very rough) approximation. For a very strong field, the magnetization is reoriented in a first-order spin-flop transition which preempts another Lifshitz transition.

In Fig. 5 we plot the temperature dependence of key thermodynamic and transport properties in phases A and B. We find that the magnetization in phase B remains essentially pinned at m_S until T becomes of the order of the gap, while it

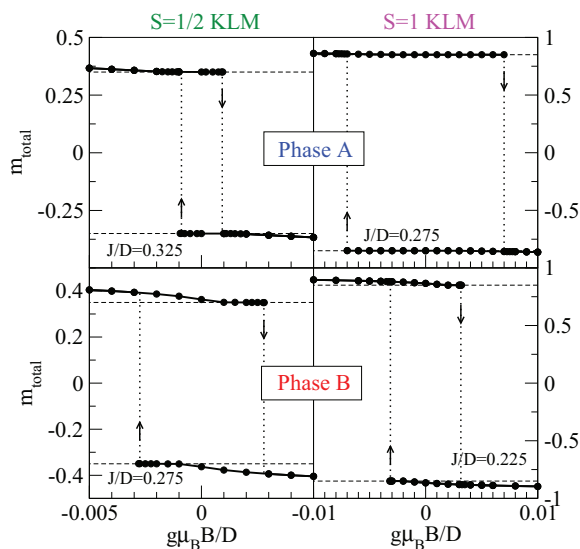


FIG. 4. (Color online) Hysteresis loops: magnetization in a longitudinal external magnetic field. The dashed lines indicate the value of the frozen magnetization m_S . The g factors are assumed equal for c and f levels, $g_c = g_f = g$. Occupancy is $n = 0.3$.

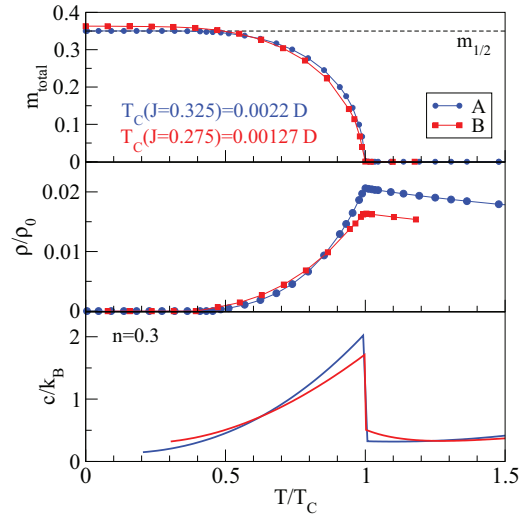


FIG. 5. (Color online) Temperature dependence of the magnetization, resistivity, and heat capacity for the spin-1/2 Kondo lattice model in phases A and B. The horizontal axis is rescaled by the Curie temperature T_C . Resistivity is in units of $\rho_0 = 2\pi e^2 \Phi(0)/\hbar D$, where Φ is the transport integral. The heat capacity curve was obtained by differentiating a piecewise interpolation of the numerical results for the total energy.

has a finite temperature derivative at $T = 0$ in phase A. This difference is, however, small. The resistance ρ increases in both phases up to the Curie temperature T_C , then it decreases approximately as a power-law $T^{-0.3}$, not logarithmically. The heat capacity c has a jump discontinuity at T_C . Similar features are indeed observed experimentally, for example in Refs. 19,22 and 23, although the simple KLM does not capture the full complexity of real materials.

C. Ferromagnetic Doniach diagram

We summarize the behavior of both Kondo lattice models in the form of a “ferromagnetic Doniach diagram” in Fig. 6. We plot the Kondo temperature for a single-impurity model with flat band (which does not depend on the impurity spin⁵⁷) and the Curie temperature T_C for each model. The Curie temperature has no observable feature at the Lifshitz transition points J^* . Apart from the (approximately) factor-of-2 difference, there is no difference in T_C of spin-1/2 and spin-1 models for small J . At large J , spin-1/2 model first goes into the B' phase and then becomes paramagnetic. The spin-1 model remains ferromagnetic in the large J limit. This

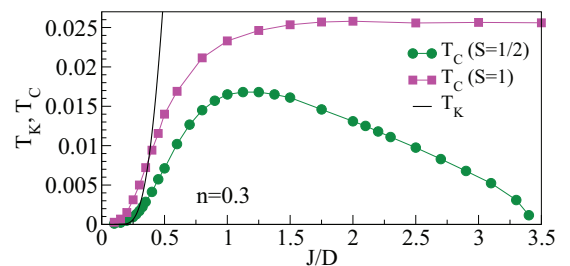


FIG. 6. (Color online) “Ferromagnetic Doniach diagram” for spin-1/2 and spin-1 Kondo lattice models.

is similar to the behavior of the AFM phases of both models at half filling.

IV. CONCLUSION

We conclude by answering the questions raised in the introduction. There is no Kondo breakdown and no criticality, but rather a continuous filling of the lower minority band and the disappearance of the electron pockets (and the emergence of hole pockets in the spin-1/2 model for large J). We find robust coexistence of FM order and Kondo screening in all phases, for both spins. Kondo underscreening does not need to be invoked to explain the magnetic ordering.

Both models have qualitatively the same phase diagram for physically most relevant small J . The Lifshitz transitions are observable in the temperature and magnetic-field dependence of the magnetization. The static mean-field appears to be valid at the qualitative level; however, to properly describe the real nature of ferromagnetic phases and transitions it is necessary to take into account dynamic effects, as in the DMFT treatment.

ACKNOWLEDGMENTS

We acknowledge discussions with Robert Peters and Janez Bonča and the support of the Slovenian Research Agency (ARRS) under Program No. P1-0044.

-
- ¹P. Coleman and A. J. Schofield, *Nature (London)* **433**, 226 (2005).
²H. Löhneysen, A. Rosch, M. Vojta, and P. Wölfle, *Rev. Mod. Phys.* **79**, 1015 (2007).
³Q. Si and F. Steglich, *Science* **329**, 1161 (2010).
⁴G. R. Stewart, *Rev. Mod. Phys.* **73**, 797 (2001).
⁵P. Gegenwart, Q. Si, and F. Steglich, *Nat. Phys.* **4**, 186 (2008).
⁶C. Pfleiderer, *Rev. Mod. Phys.* **81**, 1551 (2009).
⁷H. Tsunetsugu, M. Sigrist, and K. Ueda, *Rev. Mod. Phys.* **69**, 809 (1997).
⁸M. Gulácsi, *Adv. Phys.* **53**, 769 (2004).
⁹A. C. Hewson, *The Kondo Problem to Heavy-Fermions* (Cambridge University Press, Cambridge, 1993).
¹⁰S. Doniach, *Physica B* **91**, 231 (1977).
¹¹S. Capponi and F. F. Assaad, *Phys. Rev. B* **63**, 155114 (2001).
¹²J. Otsuki, H. Kusunose, and Y. Kuramoto, *Phys. Rev. Lett.* **102**, 017202 (2009).
¹³L. De Leo, M. Civelli, and G. Kotliar, *Phys. Rev. Lett.* **101**, 256404 (2008).
¹⁴L. C. Martin and F. F. Assaad, *Phys. Rev. Lett.* **101**, 066404 (2008).
¹⁵L. C. Martin, M. Bercx, and F. F. Assaad, *Phys. Rev. B* **82**, 245105 (2010).
¹⁶S. Süllow, M. C. Aronson, B. D. Rainford, and P. Haen, *Phys. Rev. Lett.* **82**, 2963 (1999).
¹⁷D. P. Rojas, J. I. Espeso, J. Rodríguez Fernández, J. C. Gómez Sal, J. Sanchez Marcos, and H. Müller, *Phys. Rev. B* **80**, 184413 (2009).
¹⁸K. Mukherjee, K. K. Iyer, and E. V. Sampathkumaran, *J. Phys.: Condens. Matter* **24**, 096006 (2012).
¹⁹R. E. Baumbach, H. Chudo, H. Yasuoka, F. Ronning, E. D. Bauer, and J. D. Thompson, *Phys. Rev. B* **85**, 094422 (2012).
²⁰J. Schoenes, B. Frick, and O. Vogt, *Phys. Rev. B* **30**, 6578 (1984).
²¹Z. Bukowski, R. Troć, J. Stepień-Damm, C. Sułkowski, and V. H. Tran, *J. Alloys Compd.* **403**, 65 (2005).
²²V. H. Tran, R. Troć, Z. Bukowski, D. Badurski, and C. Sułkowski, *Phys. Rev. B* **71**, 094428 (2005).
²³E. Colineau, F. Wastin, J. P. Sanchez, and J. Rebizant, *J. Phys.: Condens. Matter* **20**, 075207 (2008).
²⁴V. H. Tran, J.-C. Griveau, R. Eloirdi, W. Miiller, and E. Colineau, *Phys. Rev. B* **82**, 094407 (2010).
²⁵R. Troć, M. Samsel-Czekala, J. Stepień-Damm, and B. Coqblin, *Phys. Rev. B* **85**, 224434 (2012).
²⁶N. B. Perkins, J. R. Iglesias, M. D. Núñez-Regueiro, and B. Coqblin, *Europhys. Lett.* **79**, 57006 (2007).
²⁷N. B. Perkins, M. D. Núñez-Regueiro, B. Coqblin, and J. R. Iglesias, *Phys. Rev. B* **76**, 125101 (2007).
²⁸B. Coqblin, J. R. Iglesias, N. B. Perkins, A. S. d. R. Simoes, and C. Thomas, *Physica B: Condens. Matter* **404**, 2961 (2009).
²⁹C. Thomas, A. S. da Rosa Simões, J. R. Iglesias, C. Lacroix, N. B. Perkins, and B. Coqblin, *Phys. Rev. B* **83**, 014415 (2011).
³⁰C. Lacroix and M. Cyrot, *Phys. Rev. B* **20**, 1969 (1979).
³¹C. D. Batista, J. Bonča, and J. E. Gubernatis, *Phys. Rev. Lett.* **88**, 187203 (2002).
³²R. Peters and T. Pruschke, *Phys. Rev. B* **76**, 245101 (2007).
³³J. Otsuki, H. Kusunose, and Y. Kuramoto, *J. Phys. Soc. Jpn.* **78**, 034719 (2009).
³⁴R. Peters, N. Kawakami, and T. Pruschke, *Phys. Rev. Lett.* **108**, 086402 (2012).
³⁵K. S. D. Beach and F. F. Assaad, *Phys. Rev. B* **77**, 205123 (2008).
³⁶S. Viola Kusminskiy, K. S. D. Beach, A. H. Castro Neto, and D. K. Campbell, *Phys. Rev. B* **77**, 094419 (2008).
³⁷Y. Liu, G.-M. Zhang, and L. Yu, *Phys. Rev. B* **87**, 134409 (2013).
³⁸See Supplemental Material at <http://link.aps.org/supplemental/10.1103/PhysRevB.88.054431> for a static mean-field analysis of the spin-1/2 and spin-1 Kondo lattice models.
³⁹A. Georges, G. Kotliar, W. Krauth, and M. J. Rozenberg, *Rev. Mod. Phys.* **68**, 13 (1996).
⁴⁰K. G. Wilson, *Rev. Mod. Phys.* **47**, 773 (1975).
⁴¹R. Bulla, T. Costi, and T. Pruschke, *Rev. Mod. Phys.* **80**, 395 (2008).
⁴²W. Hofstetter, *Phys. Rev. Lett.* **85**, 1508 (2000).
⁴³R. Peters, T. Pruschke, and F. B. Anders, *Phys. Rev. B* **74**, 245114 (2006).
⁴⁴A. Weichselbaum and J. von Delft, *Phys. Rev. Lett.* **99**, 076402 (2007).
⁴⁵R. Žitko and T. Pruschke, *Phys. Rev. B* **79**, 085106 (2009).
⁴⁶K. S. D. Beach, P. A. Lee, and P. Monthoux, *Phys. Rev. Lett.* **92**, 026401 (2004).
⁴⁷K. S. D. Beach, [arXiv:cond-mat/0509778](https://arxiv.org/abs/cond-mat/0509778).
⁴⁸X. Deng, J. Mravlje, R. Žitko, M. Ferrero, G. Kotliar, and A. Georges, *Phys. Rev. Lett.* **110**, 086401 (2013).
⁴⁹R. Peters, S. Hashino, N. Kawakami, J. Otsuki, and Y. Kuramoto, *Phys. Rev. B* **87**, 165133 (2013).
⁵⁰T. Pruschke, R. Bulla, and M. Jarrell, *Phys. Rev. B* **61**, 12799 (2000).

⁵¹T. A. Costi and N. Manini, *J. Low Temp. Phys.* **126**, 835 (2002).

⁵²I. M. Lifshitz, *Sov. Phys. JETP* **11**, 1130 (1960).

⁵³Y. Yamaji, T. Misawa, and M. Imada, *J. Phys. Soc. Jpn.* **75**, 094719 (2006).

⁵⁴G.-B. Li, G.-M. Zhang, and L. Yu, *Phys. Rev. B* **81**, 094420 (2010).

⁵⁵M. Bercx and F. F. Assaad, *Phys. Rev. B* **86**, 075108 (2012).

⁵⁶R. Peters (private communication).

⁵⁷N. Andrei, K. Furuya, and J. H. Lowenstein, *Rev. Mod. Phys.* **55**, 331 (1983).